Unitary Cardiac Na^+,Ca^{2+} Exchange Current Magnitudes Determined from Channel-Like Noise and Charge Movements of Ion Transport

Donald W. Hilgemann
Department of Physiology, University of Texas Southwestern Medical Center at Dallas, Dallas, Texas 75235-9040 USA

ABSTRACT The cardiac Na^+,Ca^{2+} exchanger (NCX1) is thought to achieve a high turnover rate, but all estimates to date are indirect. Two new strategies demonstrate that maximum unitary exchange currents are about 1 fA (6000 unitary charges per s) and that they fluctuate between on and off levels similar to ion channel currents. First, exchange current noise has been identified in small cardiac patches with properties expected for a gated transport process. Noise power density spectra correlate well with exchanger inactivation kinetics, and the noise has a predicted bell-shaped dependence on the activation state of the exchanger. From the magnitudes of exchange current noise, maximum unitary exchange currents are estimated to be 0.6–1.3 fA. Second, charge movements with rates of ~5000 s^{-1} have been isolated for the transport of both Na^+ and Ca^{2+} in giant membrane patches using nonsaturating ion concentrations. The Na^+ transport reactions are disabled or "immobilized" by exchanger inactivation reactions, thus confirming that inactivation generates fully inactive exchanger states.

INTRODUCTION

The turnover rates of membrane transporters are usually estimated from measurements of transport fluxes and transporter densities under comparable conditions (e.g., Stein, 1986). For cardiac Na^+,Ca^{2+} exchange, a purely electrophysiological approach involving the analysis of current noise appears possible.

Cardiac Na^+,Ca^{2+} exchange is modulated by gating or inactivation reactions that appear to generate fully inactive exchanger states (Hilgemann et al., 1992a,b; Matsuoka and Hilgemann, 1994). Thus, single exchanger currents, if they could be measured, would be expected to fluctuate between fully on and off levels, similar to ion channel currents. Maximum Na^+,Ca^{2+} exchange rates, estimated first in cardiac vesicles (Cheon and Reeves, 1988), probably reach 5000 s^{-1} (Niggli and Lederer, 1991; Hilgemann et al., 1991; Hilgemann, 1996). This corresponds to unitary exchange currents of about 1 fA. Although a current of 1 fA is too small to resolve as a single transporter current, the ensemble fluctuations of single transporter currents can be predicted to generate significant macroscopic current noise (e.g., DeFelice, 1981; Dempster, 1993), at least in small membrane patches.

For several low-conductance channels (Zweifach and Lewis, 1994; Decoursey and Cherny, 1994; Yang and Sigworth, 1994), and for one transporter that also functions as a chloride channel (Larsson et al., 1996), analysis of current noise has allowed estimation of, or placed limits on, unitary current magnitudes in the femtoampere and subfemtoampere range. The expected function of a tightly coupled $3Na^+$-to-$1Ca^{2+}$ exchanger, which would generate macroscopic current noise, is illustrated in a minimum-state diagram in Fig. 1. Each exchanger can carry out coupled transport of three sodium ions versus one calcium ion in a consecutive exchange cycle (Läuger, 1987; Li and Kimura, 1990; Matsuoka and Hilgemann, 1992), whereby each partial reaction of this cycle might involve conformational changes equivalent to the opening or closing of an ion channel. The active fraction of exchangers would correspond to all exchangers carrying out these reactions. From the analysis of exchange current transients observed when the driving ion concentrations are changed, it was suggested that exchangers undergo an inactivation reaction specifically when three sodium ions are bound to transport sites open to the cytoplasmic side (Hilgemann et al., 1992b). The time constants of inactivation and recovery from inactivation, 1–5 s, suggest that the average dwell times of single exchangers in active and inactive states are rather long. The fraction of exchangers that are inactive in the steady-state condition can vary from <20% to >90%, depending on cytoplasmic calcium-dependent and ATP-dependent regulatory mechanisms.

An independent approach to estimating unitary exchange currents arises from measurements of exchanger charge movements associated with sodium translocation in giant membrane patches (Hilgemann et al., 1991). Charge movements recorded in response to concentration jumps depended on sodium concentrations on both membrane sides, they were sensitive to cytoplasmic calcium (and barium) concentration changes, they were inhibited by several exchange inhibitors, and they coexpressed with exchange current in *Xenopus* oocytes. The magnitudes of these charge movements suggested maximum exchanger densities of 300–400/μm^2, assuming that about one charge is moved during the translocation of three sodium ions. On this basis, maximum exchange rates of 5000/s would account for the fully activated exchange current magnitudes in excised patches. In those concentration jump experiments, the ki-

Received for publication 1 February 1996 and in final form 14 May 1996.
Address reprint requests to Dr. Donald W. Hilgemann, Department of Physiology, University of Texas Southwestern, Medical Center at Dallas, 5323 Harry Hines Boulevard, Dallas, TX 75235-9040. Tel.: 214-648-6728; Fax: 214-648-8685; E-mail: hilgeman@utsw.swmed.edu.

0006-3495/96/08/759/10 $2.00

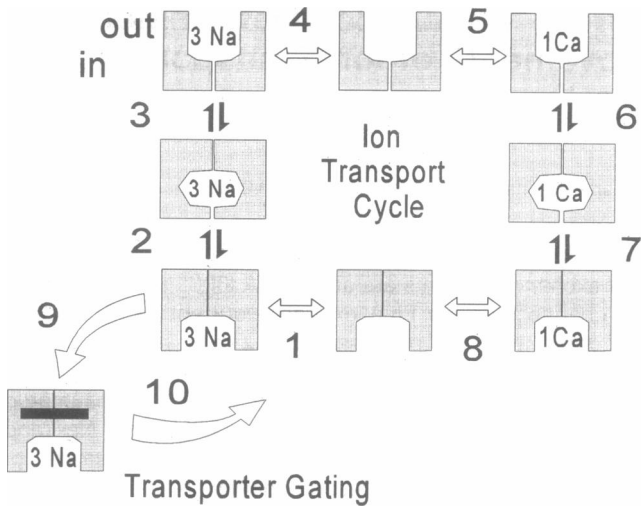

FIGURE 1 Minimum model of Na^+, Ca^{2+} exchange transport cycle with inactivation. Na^+ and Ca^{2+} transport takes place in a "consecutive" cycle. Na translocation takes place via reactions 1–4, and Ca translocation takes place via reactions 4–8. When three Na ions are bound from the cytoplasmic side, the exchanger can enter an inactive state via reaction 9. This inactivation reaction and its reversal via reaction 10 result in fluctuations of unitary exchange current and thereby generate macroscopic current noise.

netics of the underlying exchanger reactions could not be resolved.

Charge movements were not resolved for calcium transport in giant patches. However, two types of current transients were identified and suggested to involve Na, Ca exchange in experiments with caged calcium in whole myocytes. In one set of data (Niggli and Lederer, 1991), fast inward charge movements (I_{conf}) were observed and interpreted as the outward translocation of calcium, as if somewhat more than two negative binding site charges move with calcium into the membrane electrical field. These signals were increased by a nonspecific Na^+,Ca^{2+} exchange inhibitor, dichlorobenzamil, and they were not sensitive to changes in extracellular sodium or calcium or the addition of nickel. Similar exchanger densities and rates were suggested as from sodium-dependent charge movements. In another set of data (Powell et al., 1993), slower pre-steady-state current transients were recorded with calcium jumps, corresponding to a build-up of exchange current after calcium release. These charge movements were interpreted as the time course of sodium translocation, connected to an initial electroneutral translocation of calcium. The magnitudes of these results suggested exchanger densities severalfold higher than did the other studies. Consistent with Niggli and Lederer (1991), analysis of current-voltage relations for the exchange current (Matsuoka and Hilgemann, 1992) suggested that exchanger binding sites might contain three negative charges; one of them, located toward the cytoplasmic side of the transporter binding sites, would enter only partially into the membrane electrical field as the exchanger occludes cytoplasmic calcium.

Based on the results and analyses outlined, it should be possible to isolate exchanger charge movements for both sodium and calcium transport in voltage jump experiments, and it should be possible to resolve the kinetics of the underlying reactions. The giant membrane patch system is well suited for such measurements, because it allows voltage clamp of a large membrane area at rates as high as 1 MHz (Lu et al., 1995).

MATERIALS AND METHODS

Cardiac myocytes were isolated as described previously (Collins et al., 1992; Hilgemann et al., 1992b). For recordings of exchange current noise, thick-walled borosilicate glass pipettes (1.8 mm o.d.; 0.6 mm i.d) were employed. Tips were cut to 4–7-μm inner diameters (Hilgemann, 1995), melted to 2–3-μm inner diameters, and wrapped with a thick coat of a Parafilm/mineral oil/α-tocopherol mixture to reduce capacitance. Fast Fourier transforms were performed with a Hewlett-Packard 35665A dynamic signal analyzer. The pipette solution contained 100 mM tetraethylammonium (TEA) chloride, 40 mM CsCl or NaCl, 4 mM $CaCl_2$, 10 mM HEPES, and 0.3 mM ouabain. The cytoplasmic solutions contained 100 mM TEA-Cl; a total of 40 mM CsCl, LiCl, and NaCl; as indicated, 5 mM EGTA with $CaCO_3$ to achieve desired free Ca^{2+} concentrations; 10 mM HEPES; and 0.5 mM $MgCl_2$. The pH of all solutions was adjusted with TEA-OH to 7.0.

The successful resolution of low-frequency exchange current noise depended on three factors: the quality and stability of patch seals, the apparent lack of conflicting noise sources under the chosen experimental conditions, and the stability of exchange currents recorded. TEA was used as the major cation on both membrane sides because seals were more stable than with other monovalent cations. A relatively high temperature (39°C) was used to enhance rates of inactivation, thereby decreasing the stable recording time that was required for noise analysis. Pipette tip diameters of 2–3 μm were used because seal resistances (5–50 GΩ) did not improve with smaller diameters, and therefore the ratio of exchange current noise to seal noise decreased. Furthermore, exchange currents ran down over time in smaller patches. With larger pipette tips, resolution of exchange current noise was more difficult because currents were very large, relative to the current noise and background noise in the patch. Cardiac patches were used, rather than oocyte patches, because oocyte patches contain more conflicting conductances, in particular calcium-activated chloride and nonspecific conductances, which contribute noise to recordings under most conditions. The magnitudes of current noise, induced by the activation of exchange current in cardiac patches, were approximately equivalent to those induced by application of a 25-mV holding potential in the absence of exchange current.

Similar noise results were obtained with either lithium or cesium as the sodium substitute. Substitution of sodium for a 1:1 mixture of a lithium and cesium salt is, in principle, advantageous. Conductivity of the resulting solution is then very close to that of the sodium-containing solution, because lithium diffuses more slowly than sodium and cesium diffuses faster than sodium. Because 40 mM extracellular sodium has only little effect on outward exchange current with 2 or more mM extracellular calcium, the contribution of a sodium-conducting pathway, per se, to noise recordings could be tested. Noise measurements were very similar with or without 40 mM sodium in the pipette. Current noise induced by cytoplasmic sodium decreased as the exchange current ran down, and, during the same time, the current variance in the absence of sodium increased roughly proportionally to a decrease over time in seal resistance. Finally, the current variance associated with exchange activity decreased when exchange current was inhibited by pentalysine (Hilgemann and Collins, 1992), by a recently developed cyclic peptide exchange inhibitor (Khananshvilli, 1995), and by nickel in the absence of EGTA (Ehara et al,. 1989).

For charge movement recording, giant membrane patches (8–12 pF) were formed using pipettes with inner diameters of 25 to 40 μm. A modified Axopatch 200A patch clamp was employed with a 1-MHz charge

output response (Lu et al., 1995). All records were filtered at 1 MHz. Capacitance changes were monitored with 2 kHz/2 mV sinusoidal voltage perturbations at a phase angle chosen to be as insensitive as possible to membrane conductance changes (Fidler and Fernandez, 1989). Exchange current density was found to be three to four times higher in myocytes from young guinea pigs (250–250 g) than from adult guinea pigs. In fact, charge movements could be recorded reliably in cardiac membrane patches only when myocytes from young animals were employed. Fully activated outward exchange current in such patches was 100–250 pA at 37°C. The cardiac Na^+,Ca^{2+} exchanger, NCX1 (Shieh et al., 1992) was expressed in *Xenopus* oocytes as described previously (Nicoll et al., 1990).

For Na^+-dependent charge movements, the pipette solution contained 35 mM NaCl, 10 mM EGTA, 4 mM $MgCl_2$, 50 mM TEA-Cl, 50 mM CsCl, 10 mM HEPES, and 0.3 mM ouabain. For cytoplasmic solutions, $MgCl_2$ was 0.5 mM and ouabain was omitted. For Ca^{2+}-dependent charge movements, NaCl was replaced with CsCl, and 1 mM $CaCl_2$ was included in the pipette instead of EGTA. For oocyte experiments, equivalent solutions were prepared with all chloride replaced with *N*-morpholino-ethanesulfonic acid (MES) to avoid Ca^{2+}-activated chloride current. Furthermore, it was advantageous to begin oocyte patch recording only after a 10-min waiting period, during which residual chloride could diffuse from the pipette tip, and chloride currents could also dissipate by a rundown mechanism. All charge records are at 35°C, which is suitable for both oocyte and cardiac patches. Six record sets were acquired, alternatively with and without cytoplasmic exchanger ligand (Na^+ or Ca), and the averaged results were subtracted. It is noted that, initially, only fast components of charge movements were resolved in oocyte membrane, and no signals were resolved in cardiac membrane (Hilgemann, 1996). Those results were obtained at lower temperatures and with prolonged application of cytoplasmic ligands. Both factors evidently attenuate charge movements.

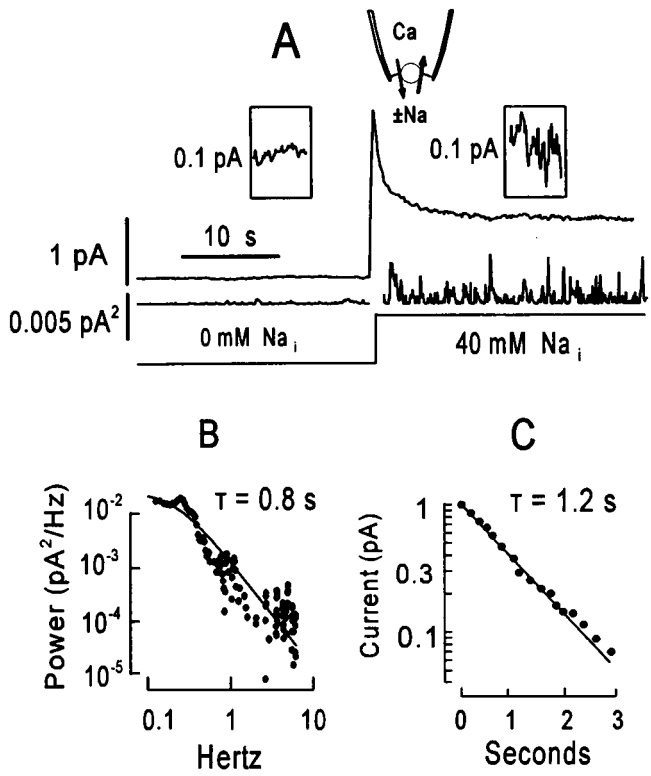

FIGURE 2 Cardiac Na^+, Ca^{2+} exchange current and current noise in a small, inside-out excised cardiac membrane patch. (*A*) Outward exchange current activated at 0 mV by replacing 20 mM LiCl + 20 mM CsCl on the cytoplasmic side with 40 mM NaCl. Here, and in subsequent figures, the pipette diagram shows schematically which ions are present. The peak current, 2.6 pA, represents nearly maximum exchange activation by Na^+. The pipette contains 40 mM NaCl with 4 mM $CaCl_2$, so the only electrochemical driving force at 0 mV is for Ca^{2+} when exchange current is activated. Variance of the current from a fitted polynomial equation is shown below the current record. Amplified portions of the current record are shown above. Signals are low-pass filtered at 10 Hz. (*B*) Power density spectrum of exchange current noise, fitted to a single Lorentzian function, $m/(1 + [f/f_c]^2)$, where f is frequency, f_c is the corner frequency, and m is a scalar variable. A power spectrum without Na^+ was subtracted from one with Na^+. The corner frequency was 0.21 Hz, giving a time constant, $1/(2 \cdot \pi \cdot f_c)$, of 0.8 s. (*C*) Logarithmic plot of the exchange current decay phase during the application of sodium. An asymptote has been subtracted, and the data points are fitted to a single exponential function with a time constant of 1.2 s.

RESULTS

Estimation of unitary exchange currents from exchange current noise

Fig. 2 shows measurements of outward Na^+,Ca^{2+} exchange current (the Ca^{2+} influx exchange mode) and exchange current noise in small cardiac membrane patches. In Fig. 2 *A*, exchange current was turned on by applying 35 mM cytoplasmic Na^+ with 4 mM Ca^{2+} in the pipette. The 2.3 pA current, which is activated initially, decays by 60% over a few seconds. Short stretches of data are amplified to illustrate the signal noise, and the variance of the current is plotted below the current record. To obtain a plot of the current variance, second-order polynomial equations were fitted to 30-s stretches of data, low-pass filtered at 10 Hz, and the squared difference of the fitted curves from the current records was calculated. The somewhat stochastic appearance of the variance record is caused by the relatively low frequency of data acquisition employed (200 Hz).

The average variance in the presence of outward exchange current, 0.0012 pA^2, is >10 times greater than background variance. Several possible sources of increased variance other than cardiac Na^+,Ca^{2+} exchange activity were eliminated. First, the increase of variance is >20 times greater than expected for the Nyquist noise of such a current. Second, the activation of exchange current does not seem to change the seal resistance significantly, because the current induced by sodium does not reverse in the voltage range of −180 to +120 mV (not shown; see Matsuoka and Hilgemann, 1992). Third, there was no increase in current noise (or current) on application of sodium when calcium was substituted for magnesium in the pipette. Fourth, the increase in noise with the application of cytoplasmic sodium was similar when 40 mM sodium was included in the pipette together with calcium. Thus, it is plausible from these results that the increase in variance could arise from fluctuations of exchangers between active and inactive states, as described for a pseudo-two-state model in Fig. 1.

For a simple two-state inactivation model, the unitary exchange current can be calculated as $\sigma^2/(I^*[1 - p])$, where σ^2 is exchange current variance, I is the steady-state current amplitude, and p is the fraction of exchangers that are active (e.g., DeFelice, 1981; Dempster, 1993). The ratio of steady-state current to peak current, 0.41, approximates p. On this

basis, the average unitary current from five experiments was 1.3 ± 0.3 fA (SEM). A possible error in this estimate arises from the fact that peak currents may not represent the activity of all exchangers. It is known, for example, that peak currents can be increased by up to twofold by increasing cytoplasmic calcium. This error leads to an overestimation of p. The largest possible error ($p \approx 0$) leads to a 41% overestimation of unitary exchange currents. Thus, these measurements would place unitary exchange currents confidently in a range of 0.6 to 1.3 fA, or 3000 to 7800 charges s^{-1}.

That the exchange current noise arises primarily from the prominent inactivation reaction, apparent in Fig. 2 *A*, is supported by the results described in Figs. 2, *B* and *C*, and 3. As shown in Fig. 2 *B*, the power density spectra of exchange current noise can be described by single Lorentzian functions under these chosen experimental conditions, as expected for the simple gating mechanism of Fig. 1. Power density spectra were calculated from stable 2-min stretches of raw current records, and the spectrum in the absence of sodium was subtracted from the spectrum in the presence of sodium. The corner frequency of the subtracted noise spectrum, 0.21 Hz, corresponds to a time constant of 0.8 s, and the average was 0.91 ± 0.14 s (SEM). If the noise arises from the same process that underlies exchange current inactivation, the time constant of inactivation should be similar. As shown in Fig. 2 *C*, the decay phase of the exchange current transient is fit well by a single exponential function, and the inactivation time constant is 1.2 s. This agrees reasonably with the time constant obtained from the power spectrum.

The power density sometimes did not have a definite plateau in the low-frequency range, particularly when lower experimental temperatures or lower free cytoplasmic calcium concentrations were employed. A sum of two or more Lorentzian functions was needed to describe such spectra, and sometimes a simple $1/f$ relationship gave a reasonable fit. On the one hand, complex spectra are not unexpected, because multiple exchanger inactivation reactions are known to modulate exchange activity (Hilgemann et al., 1992a). On the other hand, a reduction in temperature or cytoplasmic calcium lowers the time constants of the modulation reactions (Hilgemann et al., 1992a). The stability of the recordings can then be inadequate for the long data acquisition times required. For this reason, the results obtained with high experimental temperature are considered more reliable.

Treatment of the cytoplasmic membrane face with chymotrypsin largely destroys the exchanger modulation reactions and leaves the exchanger in a highly activated state. The reduction of inactivation by chymotrypsin treatment is illustrated in Fig. 3 *A* in records from a small cardiac patch. As shown in Fig. 3 *B*, the chymotrypsin treatment resulted in a large decrease in the exchange current noise, as expected if on average individual exchangers tended to operate in a continuously active fashion. Although the major effect is to scale down the power density spectrum, there is also some shift of the spectrum toward higher frequencies. Larger frequency bins were used for the spectra in Fig. 2 *B*, as compared to Fig. 1 *B*, so that all data points from the power density subtractions were positive and fell within the plotted data range.

Cytoplasmic Ca^{2+} also activates outward exchange current by a regulatory mechanism that decreases or attenuates the inactivation of exchange current (Hilgemann et al., 1992a). As shown in Fig. 3 *C*, current variance is low when exchangers are largely inactive with 0.15 μM free Ca^{2+}, it is largest when current activation is intermediate with 0.6 μM free Ca^{2+}, and it is again low when the current is highly activated with 3 μM free Ca^{2+}. These results are from a

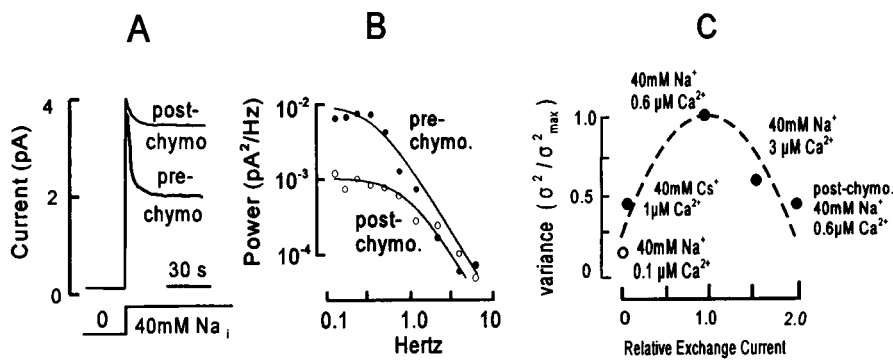

FIGURE 3 Effects of cytoplasmic chymotrypsin and Ca^{2+} on exchange current noise. (*A*) Typical exchange current records in a small cardiac patch before and after treatment of the cytoplasmic surface with 1 mg/ml chymotrypsin for 30 s. The decay of current is greatly reduced, and steady-state current is enhanced. (*B*) Power density spectra of exchange current from a small cardiac patch before and after treatment of the cytoplasmic surface with 1 mg/ml chymotrypsin for 30 s. The power spectrum is decreased after chymotrypsin. (*C*) Exchange current variance. Results are normalized to the result with 0.6 μM free Ca^{2+} with sodium. At least two measurements were averaged to give each data point, and similar results were obtained in three other patches. From left to right, data points give normalized variance in the absence of cytoplasmic Na^+ (○), with Na^+ and low free Ca^{2+} (0.15 μM), with Na^+ and 0.6 μM free Ca^{2+}, with Na^+ and 3 μM free Ca^{2+}, and with highly activated exchange current after chymotrypsin treatment. The dotted curve is a parabolic function, predicted by the hypothesis that exchange current noise arises from the calcium- and chymotrypsin-sensitive inactivation process; exchange current noise is at a maximum when about one-half of exchangers are active with 0.6 μM free Ca^{2+}.

single patch, whereby each data point represents the average of at least two determinations of current variance. The results have been normalized to the variance and current magnitudes with 40 mM sodium and 0.6 μM free Ca^{2+}. A parabolic function is plotted with the data to illustrate the predicted behavior of noise from a simple one-state model. Similar results were obtained in three other patches.

Charge movements of sodium transport

Protocols to isolate charge movements accompanying ion transport were also based on the simple model described in Fig. 1, whereby ion exchange is assumed to take place by a consecutive mechanism in which either three sodium ions or one calcium ion can be transported by the exchanger. With one ligand type (sodium or calcium) present on both membrane sides, the transport reactions (1–4 or 5–8) will be driven back and forth by changes of membrane voltage if they include voltage-dependent steps. When cytoplasmic ligand is removed, net inward ion transport should force all exchangers to a configuration with empty binding sites open to the cytoplasmic side (see Fig. 1); this is the null condition. The records presented are subtractions of null signals, acquired immediately after removal of cytoplasmic ligand, from signals obtained in the presence of cytoplasmic ligand. Charge transfer rather than current is recorded (Hilgemann, 1994), so that membrane current would be the first derivative of signals presented.

The sodium-dependent charge movements to be presented were measured after exchanger deregulation by cytoplasmic treatment with chymotrypsin to functionally remove the secondary modulation reactions. Results with patches from uninjected or water-injected oocytes showed no response with the same protocols. The ligand concentrations in all of the experiments presented are nonsaturating with respect to transport current. They were chosen because they give the best resolutions to date of the charge movements; with saturating ligand concentrations, electrogenic

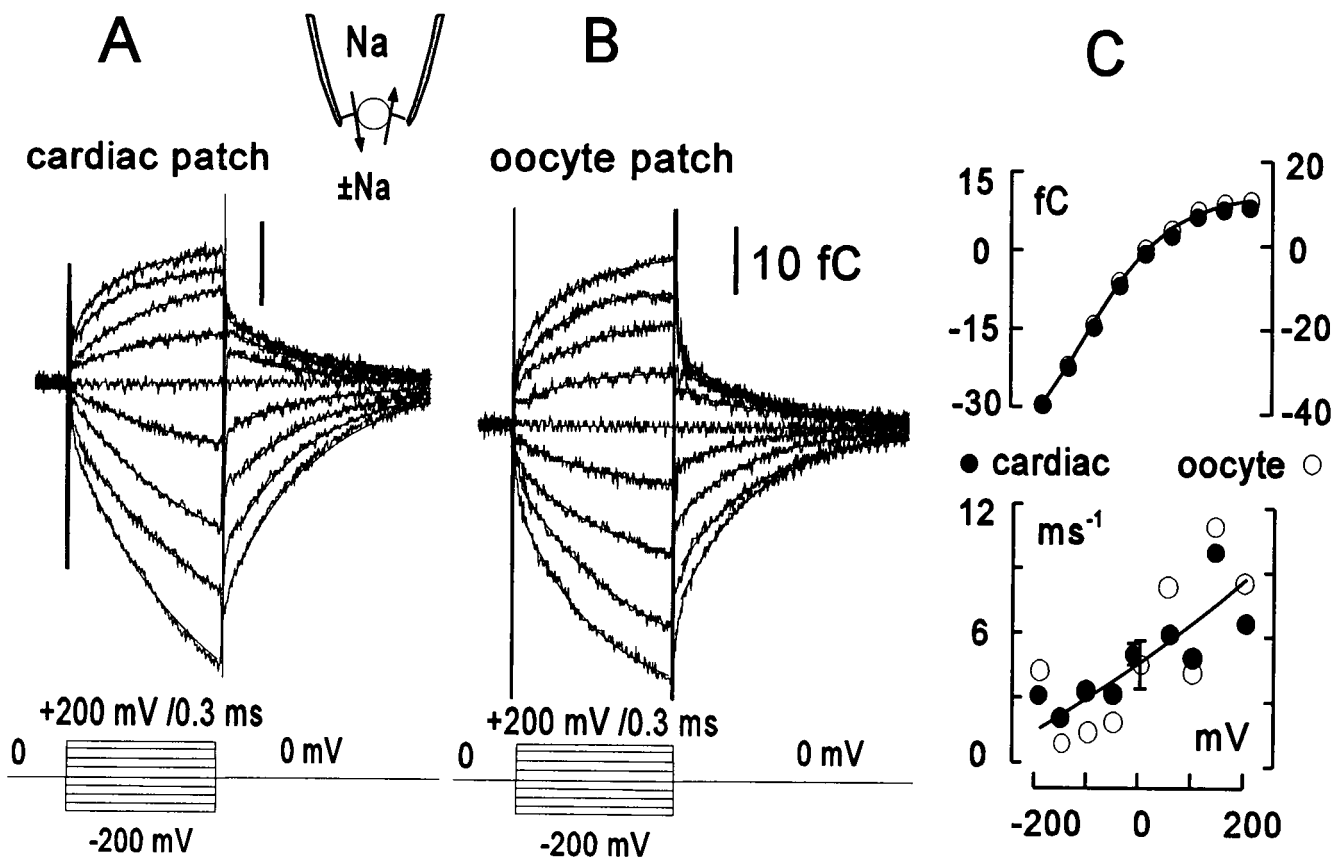

FIGURE 4 (*A* and *B*) Charge movements during Na^+ transport by chymotrypsin-treated Na^+, Ca^{2+} exchanger in a cardiac membrane patch and NCX1-expressing *Xenopus* oocyte patch, respectively. The records are subtractions of charge records without cytoplasmic Na^+ from records with 35 mM cytoplasmic Na^+. The pipette contains 35 mM Na^+ and no Ca^{2+}. Voltage steps were 0.3 ms in duration from 0 mV to positive and negative potentials in 50-mV increments. Fine lines, hardly visible, give single exponential functions, fitted to the slow signal components. The same procedures gave virtually no response in patches from uninjected oocytes. A small steady-state current that reversed near 0 mV was subtracted. This current was activated by low Na^+ and inhibited by high Na^+ concentrations, and it was similar in both cardiac and NCX1-expressing oocyte patches. It might represent, for example, a slow 2Na-to-3Na exchange mode. (*C*) Upper graph: Magnitudes of slow charge movement components during voltage steps back to 0 mV. The fitted curve is a Boltzmann function, $m/(1 + \exp([E_m - E_{50}]^*\alpha F/RT))$, where m is a scalar variable. The midpoint, E_{50}, is -75 mV, and the slope, α, is 0.36. Lower graph: Rate constants of the exponential functions fitted to charge transients. Error bars give SEM.

ion binding reactions may be missed because extreme membrane potentials are required to remove ions from binding sites.

Charge movements during Na^+ transport are presented in Fig. 4. Results for a cardiac patch are presented in Fig. 4 *A*, and the virtually indistinguishable results for an oocyte patch expressing NCX1 are presented in Fig. 4 *B*. The Na^+ concentration was 35 mM on both membrane sides. During 0.3-ms voltage pulses to large positive potentials, binding sites will be forced to open to the extracelluar side (reaction 3). Fast signal components, which appear instantaneous on return to 0 mV, probably arise from electrogenic Na^+ binding (reactions 1 and 4), similar to results for the Na^+,K^+ pump (Hilgemann, 1994). Single exponentials, fitted to slower signal components, are included as fine lines with each record. The magnitudes and rates of charge movements are plotted against pulse potential in Fig. 4 *C*. A Boltzmann equation with a slope of 0.36 fits the charge-voltage relations well. The calculated total charge moved was 60 fC, and the patch surface area was about 1000 μm^2 ($\cong$10.5 pF). Thus, 350 elementary charges are moved per μm^2, which agrees well with results from ion concentration jumps (Hilgemann et al., 1991). The rate constants of the slow charge components increase with depolarization, and the average rate at 0 mV is 5050 s^{-1}. Results for cardiac patches were indistinguishable from results for NCX1-expressing oocyte patches.

Availability of exchanger charge movements monitored as capacitance

Capacitance measurements (i.e., charge moved per change of voltage) can be used to monitor sensitively changes in the availability of charge-moving reactions (Lu et al., 1995). Briefly, membrane capacitance will appear to change whenever the magnitudes of charge movements change, if the charge movements take place faster than the voltage perturbations used to monitor capacitance. Results presented in Fig. 5 describe changes in the availability of sodium-dependent exchanger charge movements in a cardiac patch. Membrane capacitance was monitored using a 1 kHz/1 mV sinusoidal voltage perturbation. Similar to the previous charge movement measurements, the pipette contained 40 mM sodium, no added calcium, and 10 mM EGTA.

As shown in Fig. 5 *A*, the apparent membrane capacitance increases when cytoplasmic sodium is applied in the presence of extracellular sodium and in the presence of 1 μM cytoplasmic free calcium. The capacitance then decreases toward baseline over the same time course as the exchange current in equivalent records, as expected if inactivation disables the charge-moving reactions related to sodium transport. Fig. 5 *B* shows the typical absence of a capacitance response during the same protocol when cytoplasmic calcium is removed, a result equivalent to the loss of exchange current when cytoplasmic calcium is removed. As shown in Fig. 5 *C*, the capacitance response is restored,

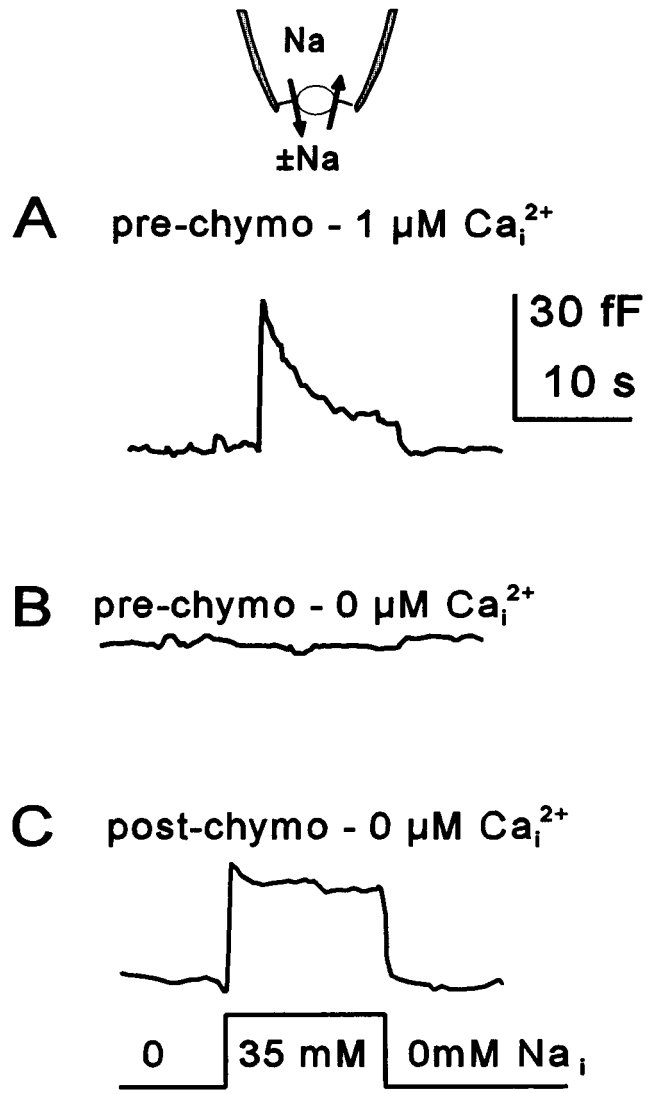

FIGURE 5 Na^+-induced capacitance changes in a cardiac membrane patch. The pipette contains 35 mM sodium, 10 mM EGTA, and no calcium. (*A*) Control response with 1 μM free cytoplasmic Ca^{2+}. When sodium is applied, capacitance increases and decreases in a waveform very similar to that of the outward exchange current when calcium instead of sodium is present in the pipette. During these responses, however, no current is activated. (*B*) Lack of response of capacitance during the application of sodium in the absence of cytoplasmic Ca^{2+}. (*C*) Capacitance response after chymotrypsin treatment in the absence of cytoplasmic Ca^{2+}. Similar results were obtained with oocyte patches expressing NCX1, whereas capacitance responses in control oocyte patches were absent during the same protocols.

becomes relatively stable, and does not require cytoplasmic calcium after treatment of the cytoplasmic membrane face with chymotrypsin. Very similar results were obtained using NCX1-expressing oocyte membrane patches (not shown). It is noted that almost no capacitance response is obtained either when sodium is removed from the pipette or when 4 mM calcium is included in the pipette. In the latter case, maximum steady-state exchange currents are activated. These results strongly support the interpretation that the capacitance changes primarily reflect changes in the

ability of sodium transport reactions to take place. The dependence of capacitance signals on extracellular sodium supports the interpretation that the predominant electrogenic reactions are closely coupled to extracellular sodium binding (Matsuoka and Hilgemann, 1992).

Equivalent capacitance measurements were performed to identify charge movements in the calcium-calcium exchange operation of the exchanger in the absence of sodium. The typical result obtained in oocyte patches expressing NCX1 is described in Fig. 6. Solution compositions were similar to those used for sodium-dependent charge movements, except for the lack of sodium and presence of calcium. Similar results were obtained with cardiac patches, but calcium-dependent capacitance signals were two- to fivefold smaller than sodium-dependent capacitance signals obtained in patches from the same myocyte batch. In Fig. 6, the extracellular (pipette) calcium concentration was 2 mM, and cytoplasmic solutions were applied with and without 1 μM free calcium. Free calcium (1 μM) causes an immediate increase in capacitance (1) of about 25 fF. Upon removal of the cytoplasmic calcium, the capacitance response typically reverses in two phases. Part of the capacitance change reverses immediately (2), and part reverses slowly with a time constant on the order of 15 s (3). It is noted that in many cases (15 recordings), capacitance did not return completely to baseline, perhaps because cytoplasmic calcium tends to increase capacitance by additional mechanisms. Importantly, the capacitance responses to cytoplasmic calcium, as well as to sodium, were inhibited by at least 70% by 20 μM dichlorobenzamil.

When experiments were performed with all extracellular calcium replaced by magnesium, an increase in capacitance was still found on application of cytoplasmic calcium (not shown), and it reversed with the slow time course of Fig. 6 (eight recordings). Thus, it can be assumed that the portion of capacitance that reverses slowly does not represent calcium binding or transport reactions. A second type of inactivation reaction of the exchanger, I_2 inactivation (Hilgemann et al., 1992a), has kinetics and dependence on cytoplasmic calcium similar to those of the slowly reversible capacitance. The I_2 inactivation might therefore be related to the slow capacitance changes. In any case, only the components of capacitance that reverse quickly on removing calcium can reflect calcium transport reactions.

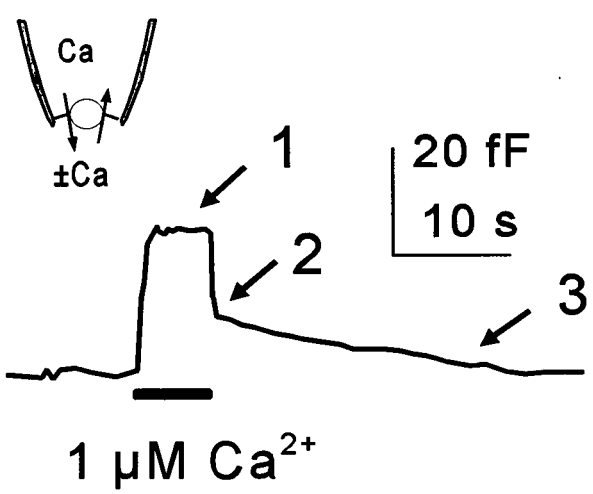

FIGURE 6 Ca^+-induced capacitance changes in an NCX1-expressing oocyte membrane patch. The extracellular calcium concentration is 2 mM, there is no sodium on either membrane side, and 1 μM free cytoplasmic calcium is applied and removed from the cytoplasmic side. The numbers represent time points at which charge signals were acquired in equivalent experiments to resolve the underlying charge movements (see Fig. 7). Note the immediate capacitance increase in response to calcium and the biphasic reversal of capacitance on removal of calcium. Similar results were obtained in the largest cardiac patches (12 pF).

Calcium-dependent exchanger charge movements

Fig. 7 describes the charge movements that underlie the fast and slow components of the Ca^{2+}-dependent capacitance changes described in Fig. 6. For the charge movement measurements, the extracellular calcium concentration was

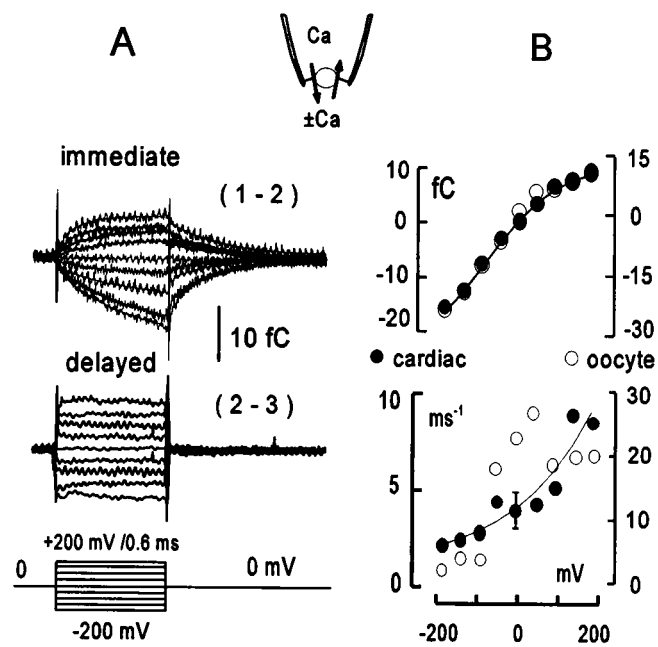

FIGURE 7 Charge movements during calcium transport by cardiac Na^+, Ca^{2+} exchange. Extracellular Ca^{2+} (1 mM) is present, there is no sodium on either membrane side, and signals are defined by application and removal of a cytoplasmic solution with 2 μM cytoplasmic free Ca^{2+}. (*A*) Charge records for 0.6-ms voltage increments from 0 mV to different potentials in 50-mV steps. The "immediate" (1–2) results are a subtraction of signals with 2 μM cytoplasmic free Ca^{2+} minus signals immediately after removal of cytoplasmic calcium. The "delayed" (2–3) results are a subtraction of signals obtained after 20 s from results immediately after removal of cytoplasmic calcium (see Fig. 6 for protocol). (*B*) Upper graph: Magnitudes of charge movements at the end of voltage steps in the 1–2′ subtraction. Results from an oocyte patch are given as open circles. The fitted Boltzmann function has a midpoint of −80 mV and a slope, α, of 0.24. Lower graph: Rate constants of the exponential functions fitted to charge transients. Error bars give SEM of the rate constants obtained for the charge transients on return to 0 mV.

1 mM and the cytoplasmic free calcium was 2 μM. Two subtractions of charge records from an NCX1-expressing oocyte patch are shown in Fig. 7 *A*. The upper records labeled "immediate" are a subtraction of charge records obtained immediately after the removal of 2 μM cytoplasmic free calcium (time point 2 in Fig. 6) from records taken in the presence of calcium (time point 1 in Fig. 6). The charge movements defined in this way are kinetically similar to the time-resolved components for the sodium-sodium exchange mode of the exchanger, but they lack pronounced fast components that appear instantaneous in these charge recordings. Similar to the capacitance signals, the calcium-dependent charge movements were three- to fourfold smaller than the sodium-dependent charge movements, recorded in the same size patches from the same oocyte batch.

The lower records in Fig. 7 *A*, labeled "delayed," show the subtraction of charge records obtained 30 s after removal of calcium (point 3 in Fig. 6 *A*) from those obtained immediately after removal of calcium (point 2 in Fig. 6 *A*). This subtraction defines a charge movement that occurs within the time needed to change voltage and which has a nearly linear dependence on voltage. This result, a linear charge movement with no time dependence, is expected for a genuine change in membrane capacitance. It is consistent with the idea that a calcium-dependent conformational change of the exchanger might increase the contribution of the exchanger to the total membrane capacitance per se.

The voltage dependencies of the immediate charge movements, which are assumed to reflect calcium transport reactions, are shown in Fig. 7 *B*. These charge movements have fast, time-resolvable components, so that the first 50 μs of records were not included in data fits to single exponentials, given as fine lines with each record. Open circles in Fig. 7 *B* give results from an oocyte patch expressing NCX1; closed circles give results for a cardiac patch. The voltage dependence of charge magnitudes and the rate constants are similar to those for Na^+ translocation. The Boltzmann slope factor for the charge-voltage relation is 0.32, and the rates of charge movements increase monotonically with depolarization. The oocyte charge movements were about twofold faster than those recorded under the same conditions in cardiac membrane. The average rate constant at 0 mV for the cardiac and the oocyte results together is 5800 s^{-1}. Note that, if these charge movements correspond to movement of a net negative charge together with calcium, the outward movement of calcium will be favored by hyperpolarization.

Estimation of exchanger turnover rates and densities from charge movements

The rates of charge movements, determined for the sodium-sodium and calcium-calcium exchange modes, can now be used to estimate an overall exchange rate within the context of the simple exchange model described in Fig. 1. In doing so, it is assumed that the slowest reactions resolved reflect the slowest steps in the exchange cycle. This is based on the idea that all reactions, including voltage-independent reactions, are in some way represented in the records for either the sodium-sodium or calcium-calcium exchange modes of the cycle. The reason is that any voltage-independent steps of the transport cycle will necessarily be in equilibrium with either sodium or calcium transport reactions. They would therefore influence the availability of the charge-moving reactions and be reflected in the kinetics charge movements. This assumption might not hold if, for example, the exchanger did not work by a consecutive mechanism.

Assuming that the slowest step of Ca^{2+} translocation (K_c) is 5800 s^{-1} and the slowest step of Na^+ translocation (K_N) is 5050 s^{-1}, an overall turnover rate can be calculated for a simple two-state consecutive carrier mechanism. With these two partial reactions taking place sequentially, the overall transport rate, $(K_c \cdot K_N)/(K_c + K_N)$, would be 2700 s^{-1}. This is somewhat lower than the maximum unitary exchange current currents estimated from noise analysis. The discrepancy is easily accounted for, however, by the fact that nonsaturating ligand concentrations were used in the charge movement measurements, and therefore the rates obtained are not maximum transport rates.

The magnitudes of charge movements can also be used to estimate the density of sodium-calcium exchangers in cardiac membrane and the unitary exchange current. To do so, it is assumed as a simplification that the total amount of charge moved by an exchanger in one cycle of transport is the charge moved during the sodium-sodium exchange charge movement plus that moved during the calcium-calcium exchange charge movement. The slopes of the Boltzmann relations are not used to estimate the amount of charge moved, because the values obtained need not reflect the amount of charge moved. A flat Boltzmann relation with a small charge coefficient can be obtained for reactions that move large amounts of charge, if multiple reactions take place in series or in parallel.

From the fitted Boltzmann relations the total amount of charge moved in the sodium-dependent plus the calcium-dependent reactions is estimated to be close to 90 fC for 10-pF patches. This corresponds to 600 charges/μm^2 of membrane (assuming 1 $\mu F/cm^2$), which is in good agreement with the previous estimate of 400 charges/μm^2 of membrane for sodium translocation alone (Hilgemann et al., 1991). The further estimation of single exchanger currents from these numbers again requires a simplification that will have to be tested in further experimentation. It must be assumed, namely, that all charge moved is related to the exchange cycle and that calcium-dependent charge movements correspond to negative charges moving in the direction opposite that of sodium translocation. Then, with maximum exchange currents of 150–300 pA in these cardiac patches, single exchanger currents of 0.25 to 0.5 pA can be extrapolated. This will be an underestimation of the single exchanger current, if part of the calcium-dependent charge movements arises from other sources (e.g., movement of positive charge into the membrane field as calcium binds).

DISCUSSION

It has been demonstrated for the first time in this article that cardiac Na^+,Ca^{2+} exchangers generate significant macroscopic current noise. Experimental conditions were selected carefully to maximize current noise by ensuring that about 50% of exchangers would be inactive in the steady state. The exchange current noise has been used to estimate the magnitudes of maximally activated unitary cardiac Na^+,Ca^{2+} exchanger currents. The estimate of 0.6 fA, to a maximum of 1.3 fA, agrees well with independent estimates of exchanger turnover rates via the isolation of exchanger charge movements for both sodium and calcium translocation. The calculation of exchanger turnover rates assumes that the exchanger moves one charge per cycle, and the estimates from charge movements assume further that the exchange process is consecutive, not simultaneous, in nature. The ability to isolate charge movements independently for sodium and calcium transport provides new support for a consecutive exchange mechanism (Läuger, 1987; Li and Kimura, 1990; Hilgemann et al., 1991; Matsuoka and Hilgemann, 1992).

Several cotransporters mediate ion movements that can be uncoupled from, or only loosely coupled to, the movement of the organic molecules transported (for overview, see DeFelice and Blakely, 1996; Cammack et al., 1994; Umbach et al., 1990; Schwartz and Tachibana, 1990; Mager et al., 1994; Galli et al., 1996; Fairman et al., 1995). Noise analysis has been used in this context to estimate the magnitudes of single transporter currents (Larsson et al., 1996) and to analyze partial transporter reactions (Cammack and Schwartz, 1996). The exchange current noise described in the present article is suggested not to arise from channel-like behavior, but rather from the gating of a tightly coupled, relatively fast $3Na^+$-to-$1Ca^{2+}$ exchange. Up to now, no uncoupled currents or ion fluxes have been identified for the cardiac Na^+,Ca^{2+} exchanger, and the reversal potentials determined for exchange current under several conditions lend support to the impression that stoichiometry of net ion transport does not deviate much from $3Na^+$-to-$1Ca^{2+}$ (Matsuoka and Hilgemann, 1992). The magnitude of exchange current noise was predicted from previous estimates of maximum exchanger turnover rates, and the power spectra of exchange current noise were predicted from the kinetics of exchange current inactivation. It seems unlikely that these correlations are coincidental.

The charge movements resolved for sodium transport by the cardiac Na^+,Ca^{2+} exchanger verify that sodium transport includes major electrogenic steps of the exchanger transport cycle; the magnitudes of sodium-dependent charge movements are severalfold greater than calcium-dependent charge movements. In comparison to results for sodium transport by the Na^+,K^+ pump (Nakao and Gadsby, 1986), the exchanger charge movements are at least 10-fold faster, they have a shallower dependence on voltage, and their rates increase rather than decrease with depolarization. Fast components of the sodium-dependent charge movements are similar, in principle, to fast components resolved for the Na^+,K^+ pump (Hilgemann, 1994). The immediate component on returning membrane potential to 0 mV from large positive potentials presumably reflects the fast binding of sodium to transport sites open to the extracellular side, as with the Na^+,K^+ pump. The immediate component observed with steps from negative voltages to 0 mV presumably reflects cytoplasmic sodium binding. The multicomponent nature of these signals is consistent with sodium transport involving multiple electrogenic steps, the most electrogenic ones probably being associated with extracellular sodium binding. A transport process comprising multiple steps, in series or parallel, can explain well the shallow voltage dependencies described previously for exchange currents (Matsuoka and Hilgemann, 1992) and now for exchanger charge movements.

The calcium-dependent charge movements resolved in the present work verify that calcium transport reactions of the cardiac Na^+,Ca^{2+} exchanger are electrogenic. It remains to be determined in charge movements what reactions are actually electrogenic. Because the charge movements are blocked by dichlorobenzamil, not enhanced, they are presumably not related to I_{conf} signals observed in caged calcium experiments in cardiac myocytes (Niggli and Lederer, 1991). Benzamil-based Na^+,Ca^{2+} exchange inhibitors block calcium-calcium exchange activity (Kaczorowski et al., 1989), and it is to be expected therefore that charge movements related to calcium transport are also blocked. Recently, caged calcium has been used to identify exchanger charge movements using giant cardiac patches, and preliminary results (Kappl and Hartung, 1996) are consistent with the magnitudes and kinetics of calcium transport-related charge movements described here.

Capacitance measurements are a highly sensitive means of identifying changes of charge-moving reactions. Because any reaction that moves charges within the membrane electrical field can contribute to these signals, it is not surprising that signal components have been identified that do not arise from ion transport reactions. The slow capacitance changes recorded on removal of cytoplasmic calcium (Fig. 6), as pointed out in the Results, have a time course consistent with an involvement of the calcium-dependent exchanger modulation reaction (termed I_2) (Hilgemann et al., 1992a). A change in the dielectric property of the exchanger protein during inactivation could explain the results. With about 500 exchangers per μm^2, and an assumed average diameter of 2 nm, the exchangers will contribute a few percent of the total membrane area, and the capacitance changes at issue are less than 0.5% of membrane capacitance. Changes in the packing of transmembrane helixes could, for example, change the dielectric properties of the exchanger protein. Still more speculatively, the inactivation reaction could involve the closure and dehydration of a pore structure formed between transmembrane exchanger domains.

In conclusion, the methods and experimental approaches described in this article suggest a wide range of further experimentation on the mechanism of sodium-calcium exchange and its "gating" via modulation reactions. That the exchanger fluctuates between active and inactive states is verified both by the existence of significant exchange current noise, with predicted dependencies on the exchanger

activation state, and by the fact that charge movements related to sodium transport are disabled or immobilized by the exchanger inactivation reaction. That maximum transport rates of single Na^+,Ca^{2+} exchangers are in the range of 5000 s^{-1} is now independently verified by 1) the identification and analysis of exchange current noise, and 2) the independent resolution of charge movements associated with sodium and calcium transport reactions.

I thank L. J. DeFelice, D. C. Gadsby, and C. M. Baud for thoughtful criticism and encouragement; C.-C. Lu and A. Kabakov for discussions and providing cells; S. Feng for technical assistance; R. P. Malchow for helpful comments on the manuscript; and K. D. Philipson and D. A. Nicoll for providing cRNA for NCX1.

This work was supported by grants from the National Institutes of Health (5-R1-HL51323-03) and the American Heart Association (95014830).

REFERENCES

Cammack, J. N., S. V. Rakhilin, and E. A. Schwartz. 1994. A GABA transporter operates asymmetrically with variable stoichiometry. *Neuron.* 13:949–960.

Cammack, J. N., and E. A. Schwartz. 1996. Channel behavior in a gamma-aminobutyrate transporter. *Proc. Natl. Acad. Sci. USA.* 93:723–727.

Cheon, J., and J. P. Reeves. 1988. Site density of the sodium-calcium exchange carrier in reconstituted vesicles from bovine cardiac sarcolemma. *J. Biol. Chem.* 263:2309–2315.

Collins, A., A. Somlyo, and D. W. Hilgemann. 1992. The giant cardiac membrane patch method: stimulation of outward Na^+/Ca^{2+} exchange current by MgATP. *J. Physiol. (Lond.).* 454:37–57.

Decoursey, T. E., and V. V. Cherny. 1994. Voltage-activated hydrogen ion currents. *J. Membr. Biol.* 141:203–215.

DeFelice, L. J. 1981. Introduction to Membrane Noise. Plenum Press, New York.

DeFelice, L. J., and R. D. Blakely. 1996. Pore models for transporters? *Biophys. J.* 70:579–580.

Dempster, J. 1993. Computer Analysis of Electrophysiological Signals. Academic Press, London.

Ehara, T., S. Matsuoka, and A. Noma. 1989. Measurement of reversal potential of Na^+-Ca^{2+} exchange current in single guinea-pig ventricular cells. *J. Physiol. (Lond.).* 410:227–249.

Fairman, W. A., R. J. Vandenberg, J. L. Arriza, M. P. Kavanaugh, and S. G. Amara. 1995. An excitatory amino acid transporter with properties of a ligand-gated chloride channel. *Nature.* 375:599–602.

Fidler, N., and J. M. Fernandez. 1989. Phase tracking: an improved phase detection technique for cell membrane capacitance measurements. *Biophys. J.* 56:1153–1162.

Galli, A., R. D. Blakely, and L. J. DeFelice. 1996. NETs have channel modes of conduction. *Proc. Natl. Acad. Sci. USA.* In press.

Hilgemann, D. W. 1994. Channel-like function of the Na, K pump probed at microsecond resolution in giant membrane patches. *Science.* 263: 1429–1432.

Hilgemann, D. W. 1995. The giant membrane patch. *In* Single Channel Recording. B. Sakmann and E. Neher, editors. Plenum Press, New York. 307–327.

Hilgemann, D. W. 1996. The cardiac sodium-calcium exchanger in giant membrane patches. *Ann. N.Y. Acad. Sci.* 779:136–158.

Hilgemann, D. W., and A. Collins. 1992. The mechanism of sodium-calcium exchange stimulation by ATP in giant cardiac membrane patches: possible role of aminophospholipid translocase. *J. Physiol. (Lond.).* 454:59–82.

Hilgemann, D. W., A. Collins, and S. Matsuoka. 1992a. Dynamic and steady state properties of cardiac sodium-calcium exchange: calcium- and ATP-dependent activation. *J. Gen. Physiol.* 100:933–961.

Hilgemann, D. W., S. Matsuoka, G. A. Nagel, and A. Collins. 1992b. Dynamic and steady state properties of cardiac sodium-calcium exchange: sodium-dependent inactivation. *J. Gen. Physiol.* 100: 905–932.

Hilgemann, D. W., D. A. Nicoll, and K. D. Philipson. 1991. Charge movement during sodium translocation by native and cloned cardiac Na^+/Ca^{2+} exchanger in giant excised membrane patches. *Nature.* 352: 715–719.

Kaczorowski, G. J., M. L. Barcia, V. F. King, and R. S. Slaughter. 1989. Development and use of inhibitors to study sodium-calcium exchange. *In* Sodium-Calcium Exchange. T. J. A. Allen, D. Noble, and H. Reuter, editors. Oxford University Press, New York. 66–101.

Kappl, M., and K. Hartung. 1996. Kinetics of Na-Ca exchange current after a Ca^{2+} concentration jump. *Ann. N.Y. Acad. Sci.* 779:290–292.

Khananshvilli, D. 1995. Positively charged cyclic hexapeptides, novel blockers for the cardiac sarcolemma Na^+-Ca^{2+} exchanger. *J. Biol. Chem.* 270:16182–16188.

Larsson, H. J. P., S. A. Picaud, F. S. Werblin, and H. Lecar. 1996. Noise analysis of the glutamate-activated current in photoreceptors. *Biophys. J.* 70:733–742.

Läuger, P. 1987. Voltage dependence of sodium-calcium exchange: predictions from kinetic models. *J. Membr. Biol.* 99:1–12.

Li, J., and J. Kimura. 1990. Translocation mechanism of cardiac Na^+-Ca^{2+} exchange in single cardiac cells of guinea pig. *J. Gen. Physiol.* 96: 777–788.

Lu, C.-C., A. Kabakov, S. Mager, V. Markin, G. Frazier, and D. W. Hilgemann. 1995. Membrane transport mechanisms probed by capacitance measurements with megahertz voltage clamp. *Proc. Natl. Acad. Sci. USA.* 92:11220–11224.

Mager, S., C. Min, D. J. Henry, C. Chavkin, B. J. Hoffman, N. Davidson, and H. Lester. 1994. Conducting states of a mammalian serotonin transporter. *Neuron.* 12:845–859.

Matsuoka, S., and D. W. Hilgemann. 1992. Dynamic and steady state properties of cardiac sodium-calcium exchange: ion and voltage dependencies of transport cycle. *J. Gen. Physiol.* 100:962–1001.

Matsuoka, S., and D. W. Hilgemann. 1994. Inactivation of outward Na/Ca exchange current in guinea pig ventricular myocytes. *J. Physiol. (Lond.).* 476:443–458.

Nakao, M., and D. C. Gadsby. 1986. Voltage dependence of Na translocation by the Na/K pump. *Nature.* 323:628–630.

Nicoll, D. A., S. Longoni, and K. D. Philipson. 1990. Molecular cloning and functional expression of the cardiac sarcolemmal Na^+-Ca^{2+} exchanger. *Science.* 250:562–565.

Niggli, E., and W. J. Lederer. 1991. Molecular operations of the sodium-calcium exchanger revealed by conformation currents. *Nature.* 349: 621–623.

Powell, T., A. Noma, T. Shioya, and R. Z. Kozlowski. 1993. Turnover rate of the cardaic Na^+-Ca^{2+} exchanger in guinea pig ventricular myocytes. *J. Physiol. (Lond.).* 472:45–53.

Schwartz, E. A., and M. Tachibana. 1990. Electrophysiology of glutamate and sodium cotranpsort in a glial-cell of the salamander retina. *J. Physiol. (Lond.).* 426:43–80.

Shieh, B. H., Y. Xia, R. S. Sparkes, I. Klisak, A. J. Lusis, D. A. Nicoll, and K. D. Philipson. 1992. Mapping of the gene for the cardiac sarcolemmal Na^+-Ca^{2+} exchanger to human chromosome 2p21–p23. *Genomics.* 12: 616.

Stein, W. D. 1986. Transport and Diffusion Across Cell Membranes. Academic Press, San Diego.

Umbach, J. A., M. J. Coady, and E. M. Wright. 1990. Intestinal Na^+/glucose cotransporter expressed in *Xenopus* oocytes is electrogenic. *Biophys. J.* 57:1217–1224.

Yang, Y., and F. J. Sigworth. 1994. The conductance of MinK "channels" is very small. *Biophys. J.* 68:A22.

Zhaoping, L., D. A. Nicoll, D. W. Hilgemann, A. Collins, J. T. Penniston, J. Tomich, J. N. Weiss, and K. D. Philipson. 1991. Identification of a peptide inhibitor of the cardiac sarcolemmal Na/Ca Exchanger. *J. Biol. Chem.* 266:1014–1020.

Zweifach, A., and R. S. Lewis. 1994. Mitogen-regulated Ca^{2+} current of T-lymphocytes is activated by depletion of intracellular Ca^{2-} stores. *Proc. Natl. Acad. Sci. USA.* 90:6295–6300.